Electronic Supplementary Material (ESI) for Physical Chemistry Chemical Physics.

Supporting Information for

Ionic Liquid Crystals-Based Solid Organic Electrolytes for Li Ion Batteries: Experiments and Modeling

Md Sharif Khan[1], Ambroise Van Roekeghem[1], Stefano Mossa[2], Flavien Ivol[1], Laurent Bernard[1], Lionel Picard[1] and Natalio Mingo[1]**

[1]*Université Grenoble Alpes, CEA, LITEN, 17 rue des Martyrs, 38054 Grenoble Cedex 9, France*

[2]*Université Grenoble Alpes, CEA, IRIG-MEM, 17 rue des Martyrs, 38054 Grenoble Cedex 9, France*

Corresponding Author

* E-mail: sharifkhanjnu@gmail.com

* E-mail: natalio.mingo@cea.fr

Figures S1 –S13

Molecular design considerations and synthesis

For clarity, we use a reduced nomenclature, which includes the anion (or its abbreviation), a dash and the lengths of the two alkyl chains present in the cation, separated by a comma. For example, the label BS-12-H refers to the derivative 4-(didodecylamino) naphthalene-1-sulfonic acid. The formation of the target compound is schematically represented in Scheme S1.

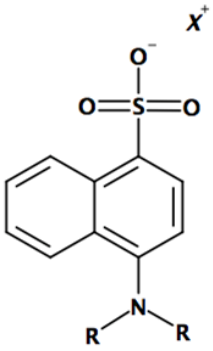

Figure S1 : Representation of the model molecule containing: a cation X^+, an anion, a mesogen group and alkyl chains

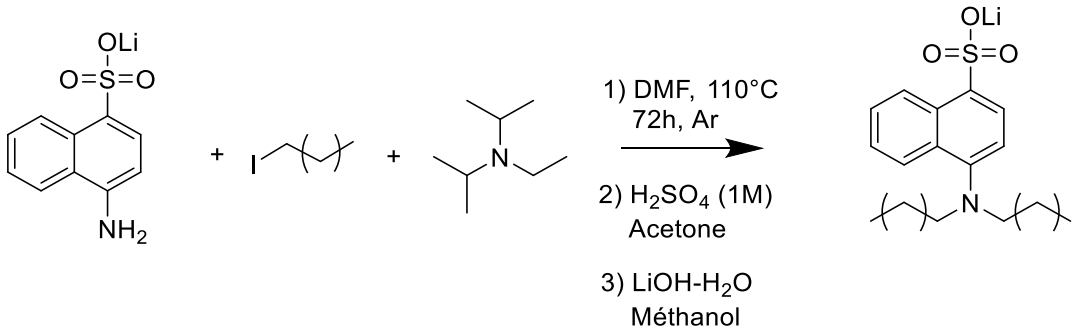

Scheme S1 : General synthesis protocol

The chain lengths differ by the number of alkyl groups in the chain from 8, 12, and 16, namely lithium 4 - (dioctylamino) naphthalene - 1 - sulfonate (BS-Li-8), lithium 4 - (didodecylamino) naphthalene - 1 - sulfonate (BS-Li-12), and lithium 4 - (dihexadecylamino) naphthalene - 1 - sulfonate (BS-Li-16).

The 4-amino-1-naphtalenesulfonic acid (ANH) (97%) was commercially obtained from Sigma-Aldrich. The lithium-4-amino-1-naphtalenesulfonate (ANLi) was prepared by an ion exchange from the acid form to the lithium salt using lithium hydroxide monohydrate (LiOH.H2O). An equimolar amount of LiOH and ANH are introduced in deionized water : ANH was not soluble in water while ANLi was. The reaction mixture was stirred for 24 h at room temperature. The excess of ANH was removed by filtration. Finally, the solution was freeze-dried in a lyophiliser at - 90 °C for 48 hours until all water sublimated. the resulted powder was the desired product. Then, the solid was dried overnight in a vacuum oven (10 mbar) at 70 °C to remove the last traces of water, prior to NMR characterization :

^{1}H NMR (400.13 MHz, DMSO- d_6, 298.15 K) δ 8.73 (d, J = 8 Hz, 1 H), δ 8.03 (d, J = 8 Hz, 1 H), δ 7.66 (d, J = 8.0 Hz, 1 H), δ 7.36 (q, J = 4.0 Hz, 2 H), δ 6.51 (d, J = 8.0 Hz, 1 H), δ 5.80 (s, 2 H) ppm

^{13}C NMR (400.13 MHz, DMSO- d_6, 298.15 K) δ 146.19 (1 C), δ 132.61 (1 C), δ 130.76 (1 C), δ 128.28 (1 C), δ 126.54 (1 C), δ 125.45 (1 C), δ 123.68 (1 C), δ 123.08 (1 C), δ 122.39 (1 C), δ 105.31 (1 C) ppm

^{7}Li NMR (400.13 MHz, DMSO- d_6) δ -1.05 ppm

The lithium-4-amino-1-naphtalenesulfonate (ANLi) (1 eq.) and N, N-diisopropylethylamine (DIPEA) (3.10 eq.) were solubilized in dry dimethylformamide (DMF) followed by the addition, under argon atmosphere and constant stirring, of the iodio-alkyles (1-iodooctane C_8 ; 1-iodododecane C_{12} ; 1-Iodohexadecane C_{16}) (2.70 eq.) according to desired chain length. The reaction mixture was stirred for 72 hours at 110 °C in order to achieve the greatest conversion and the progress of the reaction was monitored by thin layer chromatography using dichloromethane as mobile phase. After completion of the reaction, as indicated by the disappearance of the reactant spots, the reaction solution was precipitated in 1M H_2SO_4 : acetone

(10 : 1) and stirred for 2 hours at room temperature. The resulting solid was then filtered through a Büchner funnel, and then washed with acetone first and then by pentane and finally, it was recrystallized from methanol to get the desired disubstituted product in the protonic form. A white pure crystalline powder is obtained with an isolated yield around 85 - 90%. The product was finally dried overnight in a vacuum oven (10 mbar) at 110 °C prior to NMR characterization :

BS-8-H

^{1}H NMR (400.13 MHz, DMSO- d_6, 298,15 K) δ 8.82 (d, J = 8.0 Hz, 1 H), δ 8.21 (d, J = 8.0 Hz, 1 H), δ 7.86 (d, J = 8.0 Hz, 1 H), δ 7.45 (q, J = 4.0 Hz, 2 H), δ 7.11 (d, J = 8.0 Hz, 1 H), δ 3.07 (t, J = 8.0 Hz, 4 H), δ 1.42 (q, J = 8.0 Hz, 4 H), δ 1.19 (m, 20 H), δ 0.82 (t, J = 8.0 Hz, 6 H) ppm

^{13}C NMR (400.13 MHz, DMSO- d_6, 298,15 K) δ 148.81 (1 C), δ 139.19 (1 C), δ 130.46 (1 C), δ 130.41 (1 C), δ 128.05 (1 C), δ 125.14 (1 C), δ 124.62 (1 C), δ 124.35 (1 C), δ 123.26 (1 C), δ 116.05 (1 C), δ 53.41 (2 C), δ 31.08 (2 C), δ 28.63 (2 C), δ 28.54 (2 C), δ 26.56 (2 C), δ 26.36 (2 C), δ 21.94 (2 C,) δ 13.84 (2 C) ppm

ESI/MS : m/z 446 [M-H]-

BS-12-H

^{1}H NMR (400.13 MHz, DMSO- d_6, 298,15 K) δ 8.81 (d, J = 8.0 Hz, 1 H), δ 8.20 (d, J = 8.0 Hz, 1 H), δ 7.85 (d, J = 8.0 Hz, 1 H), δ 7.44 (q, J = 4.0 Hz, 2 H), δ 7.11 (d, J = 8.0 Hz, 1 H), δ 3.06 (t, J = 8.0 Hz, 4 H), δ 1.42 (q, J = 8.0 Hz, 4 H), δ 1.19 (m, 36 H), δ 0.85 (t, J = 8.0 Hz, 6 H) ppm

^{13}C NMR (400.13 MHz, DMSO- d_6, 298,15 K) δ 148.76 (1 C), δ 139.08 (1 C), δ 130.41 (1 C), δ 130.35 (1 C), δ 128.00 (1 C), δ 125.07 (1 C), δ 124.53 (1 C), δ 124.35 (1 C), δ 123.22 (1 C), δ 116.02 (1 C), δ 53.32 (2 C), δ 31.21 (2 C), δ 28.64 (5 C), δ 28.60 (5 C), δ 26.53 (4 C), δ 26.37 (2 C), δ 22.01 (2 C), δ 13.86 (2 C) ppm

ESI/MS : m/z 558 [M-H]-

BS-16-H

^{1}H NMR (400.13 MHz, DMSO- d_6, 298,15 K) δ 8.81 (d, J = 8.0 Hz, 1 H), δ 8.20 (d, J = 8.0 Hz, 1 H), δ 7.85 (d, J = 8.0 Hz, 1 H), δ 7.44 (q, J = 4.0 Hz, 2 H), δ 7.11 (d, J = 8.0 Hz, 1 H), δ 3.05 (t, J = 8.0 Hz, 4 H), δ 1.42 (q, J = 8.0 Hz, 4 H), δ 1.20 (m, 52 H), δ 0.85 (t, J = 8.0 Hz, 6 H) ppm

^{13}C NMR (400.13 MHz, DMSO- d_6, 298,15 K) δ 148.93 (1 C), δ 139.20 (1 C), δ 130.57 (1 C), δ 130.48 (1 C), δ 128.15 (1 C), δ 125.22 (1 C), δ 124.68 (1 C), δ 124.12 (1 C), δ 123.10 (1 C), δ 115.70 (1 C), δ 53.04 (2 C), δ 31.02 (2 C), δ 28.95 (9 C), δ 28.90 (9 C), δ 26.51 (4 C), δ 26.36 (2 C), δ 22.01 (2 C), δ 13.86 (2 C) ppm

ESI/MS : m/z 685 [M-H]-

An ion exchange from the proton to the lithium form was then performed. The protonated disubstituted product (1 eq.) were lithiated with lithium hydroxide (1 eq.) in methanol under argon atmosphere. The slurry was stirred for 2 hours at room temperature and the crude product was concentrated by evaporation of the solvent under reduced pressure. Then, before being stored in a glovebox, the final materials were dried overnight in a vacuum oven (10 mbar) at 110 °C and characterized by NMR.

BS-8-Li

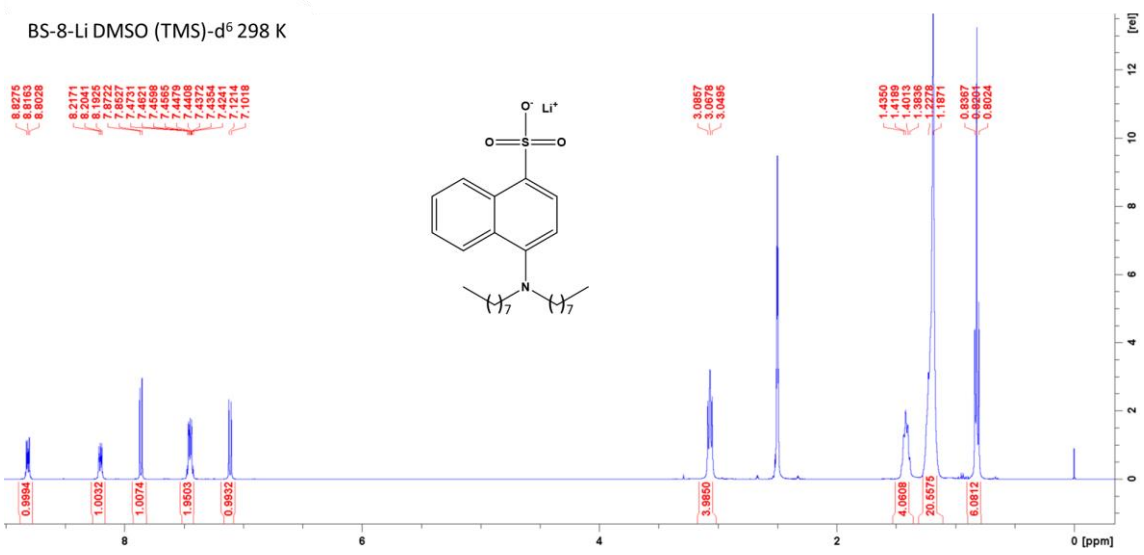

Figure S2: ^{1}H NMR spectrum of BS-8-Li

^{1}H NMR (400.13 MHz, DMSO- d_6, 298,15 K) δ 8.81 (d, J = 8.0 Hz, 1 H), δ 8.20 (d, J = 8.0 Hz, 1 H), δ 7.86 (d, J = 8.0 Hz, 1 H), δ 7.46 (q, J = 4.0 Hz, 2 H), δ 7.11 (d, J = 8.0 Hz, 1 H), δ 3.06 (t, J = 8.0 Hz, 4 H), δ 1.41 (q, J = 8.0 Hz, 4 H), δ 1.17 (m, 20 H), δ 0.80 (t, J = 8.0 Hz, 6 H) ppm

^{13}C NMR (400.13 MHz, DMSO- d_6, 298,15 K) δ 148.75 (1 C), δ 139.13 (1 C), δ 130.40 (1 C), δ 130.35 (1 C), δ 127.99 (1 C), δ 125.08 (1 C), δ 124.56 (1 C), δ 124.34 (1 C), δ 123.25 (1 C), δ 116.04 (1 C), δ 53.39 (2 C), δ 31.10 (2 C), δ 28.66 (2 C), δ 28.57 (2 C), δ 26.59 (2 C), δ 26.38 (2 C), δ 21.95 (2 C), δ 13.84 (2 C) ppm

^{7}Li NMR (400.13 MHz, DMSO- d_6) δ -1.06 ppm

BS-12-Li

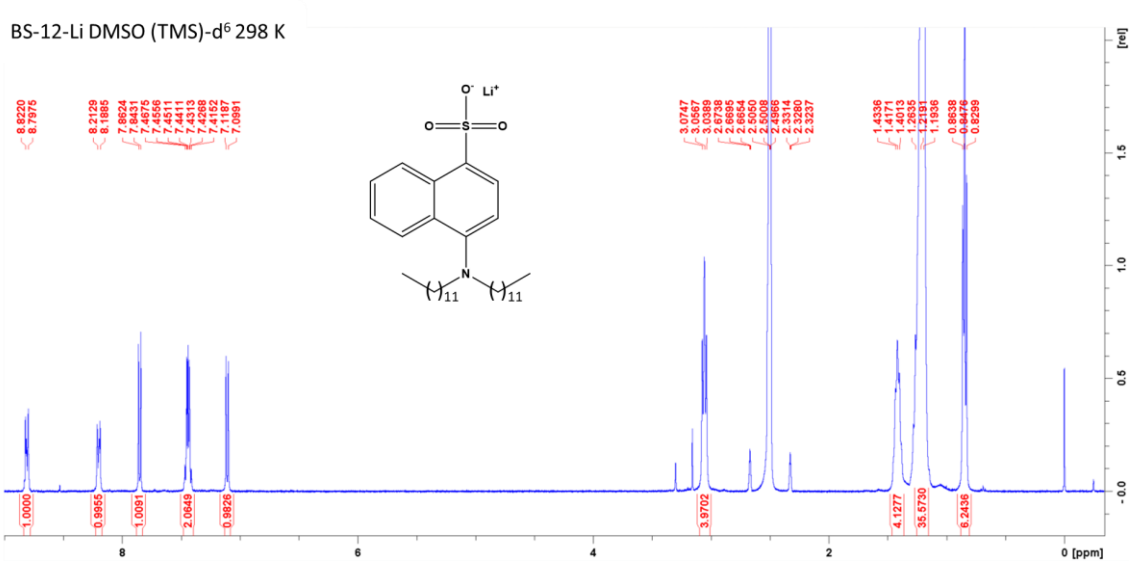

Figure S3: ^{1}H NMR spectrum of BS-12-Li

^{1}H NMR (400.13 MHz, DMSO- d_6, 298,15 K) δ 8.82 (d, J = 8.0 Hz, 1 H), δ 8.21 (d, J = 8.0 Hz, 1 H), δ 7.86 (d, J = 8.0 Hz, 1 H), δ 7.44 (q, J = 4.0 Hz, 2 H), δ 7.11 (d, J = 8.0 Hz, 1 H), δ 3.06 (t, J = 8.0 Hz, 4 H), δ 1.42 (q, J = 8.0 Hz, 4 H), δ 1.20 (m, 36 H), δ 0.85 (t, J = 8.0 Hz, 6 H) ppm

^{13}C NMR (400.13 MHz, DMSO- d_6, 298,15 K) δ 148.80 (1 C), δ 139.12 (1 C), δ 130.39 (1 C), δ 130.33 (1 C), δ 127.98 (1 C), δ 125.05 (1 C), δ 124.51 (1 C), δ 124.33 (1 C), δ 123.20 (1 C), δ 116.00 (1 C), δ 53.30 (2 C), δ 31.20 (2 C), δ 28.89 (5 C), δ 28.59 (5 C), δ 26.52 (4 C), δ 26.36 (2 C), δ 21.99 (2 C), δ 13.84 (2 C) ppm

^{7}Li NMR (400.13 MHz, DMSO- d_6, 298.15 K) δ -1.04 ppm

BS-16-Li

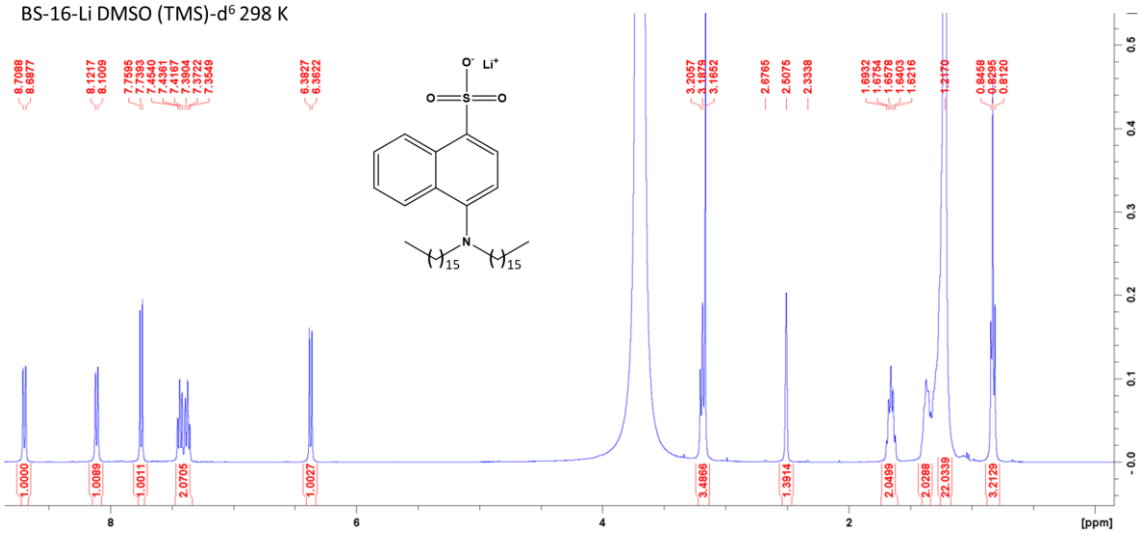

Figure S4: [1]H NMR spectrum of BS-16-Li

[1]H NMR (400.13 MHz, DMSO- d_6, 298,15 K) δ 8.81 (d, J = 8.0 Hz, 1 H), δ 8.22 (d, J = 8.0 Hz, 1 H), δ 7.86 (d, J = 8.0 Hz, 1 H), δ 7.41 (q, J = 4.0 Hz, 2 H), δ 6.47 (d, J = 8.0 Hz, 1 H), δ 3.19 (t, J = 8.0 Hz, 4 H), δ 1.37 (q, J = 8.0 Hz, 4 H), δ 1.22 (m, 52 H), δ 0.83 (t, J = 8.0 Hz, 6 H) ppm

[13]C NMR (400.13 MHz, DMSO- d_6, 298,15 K) δ 148.88 (1 C), δ 139.15 (1 C), δ 130.43 (1 C), δ 130.34 (1 C), δ 128.01 (1 C), δ 125.06 (1 C), δ 124.93 (1 C), δ 124.37 (1 C), δ 123.32 (1 C), δ 115.92 (1 C), δ 53.26 (2 C), δ 31.24 (2 C), δ 28.74 (9 C), δ 28.66 (9 C), δ 26.51 (4 C), δ 26.39 (2 C), δ 22.04 (2 C), δ 13.87 (2 C) ppm

[7]Li NMR (400.13 MHz, DMSO- d_6) δ -1.03 ppm

The [1]H NMR and [13]C NMR spectra of the compounds of the series BS-(8/12/16)-Li, recorded in DMSO - d_6 solution at room temperature, showed well-defined peaks associated with the aromatic and aliphatic protons of the alkyls chains. The aromatic signals are not significantly altered by the alkyls chains. The aromatic proton exhibit similar chemical shift values independently of the chain lengths, which could be attributed to the determinant effect produced by the S atom of the respective anion in the interactions with the cation. The [7]Li-NMR spectra of the all compounds,

recorded in DMSO - d_6 solution at room temperature, exhibit a single peak around -1.04 ppm, in agreement with the presence of the lithium cation.

Electrochemical Impedance Spectroscopy (EIS) Measurement:

In the Ar purged glovebox, the symmetric cells were fabricated using CR2032 coin cells. The compounds, in the solid powder form (white colour), were sandwiched between two stainless steel electrodes with an inner diameter of the brace of 15 mm (high surface to thickness ratio). The samples were heated up to their isotropization temperature, temperature at which a good interface is formed and then cooled down. The coin cell was then inspected for ensuring the absence of leaks around the brace.

EIS measurements were performed using a Bio-Logic electrochemical workstation and a temperature controller. The environmental chamber were turned on and allowed to come to equilibration/operational temperatures for 30 min prior to the start of measurements. Each temperature change was accompanied by a variable time period (heating/cooling dependent) in which the instrument was allowed to reach the new set-point until it was within ± 0.3 °C and then stabilized for 30 min prior to measurement. Each tested material remained undisturbed in the environmental chamber for the duration of the variable temperature testing. All the testing cables were shielded.

In the EIS method for determining the ionic conductivity, a sinusoidal electrical potential is imposed to the sample for different frequencies, and the resulting current is measured to determine the impedance (Z) of the sample (both the imaginary and real components). The frequencies sweep from 7 MHz - 1 Hz with a voltage amplitude of 70 mV for each temperature. The sample were recorded upon heating and cooling between 20 and 80 °C (accuracy: ± 0.3 °C after

stabilization). The measures were taken under steady state conditions, where the selected T was stabilized for 30 min before taking impedance measurements over the full frequency-range.

The obtained EIS data did not fit a typical Randles-type RC-series circuit model because of the nontraditional structure of this electrolyte materials. The Nyquist plot shows only one process, a high frequency attributed to the bulk resistance. The bulk resistance (R) was determined from the Nyquist plot, by taking the interception point between the semi-circle (i.e. low frequency relaxation of less than 1 Hz) and the real part of the impedance Z'. The semicircle represents the dielectric contribution, where the diameter of the semicircle corresponds to the resistance (R) of the charge transport within the material.

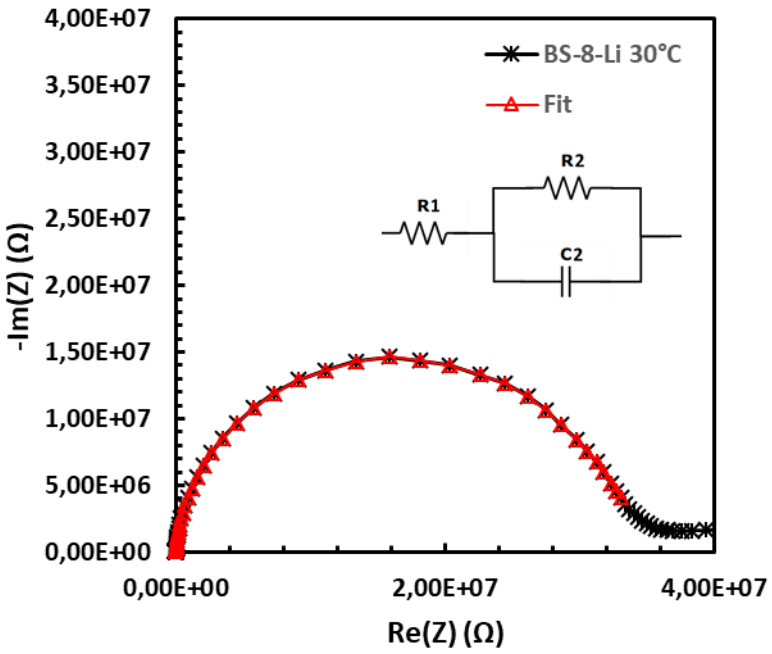

Figure S5: Example of Nyquist plot measured for BS-8-Li at 40°C and the associated fit with the equivalent circuit used.

Thermal stability evaluation by TGA:

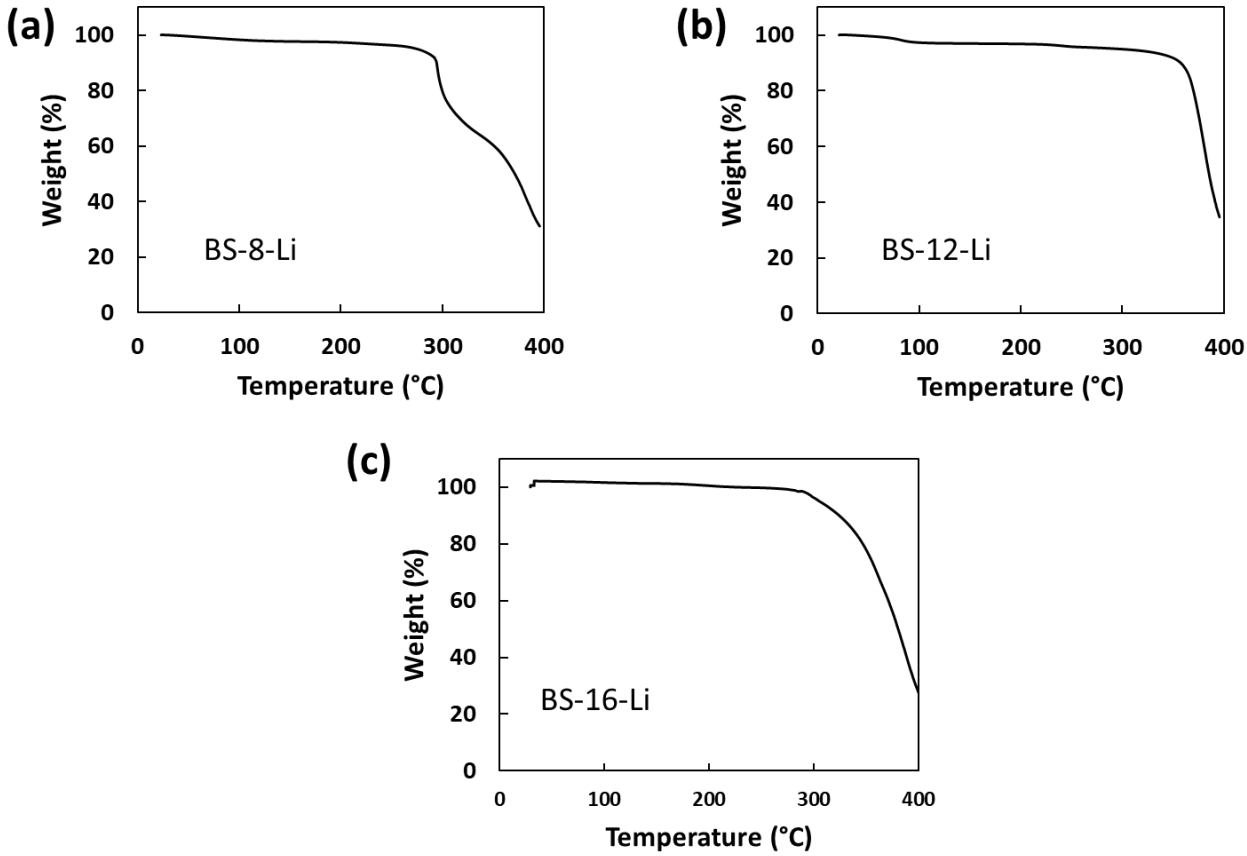

Figure S6 : (a) TGA curve of BS-8-Li measured at 5 °C.min^{-1} under He-atmosphere (b) TGA curve of BS-12-Li measured at 5 °C.min^{-1} under He-atmosphere (c) TGA curve of BS-16-Li measured at 5 °C.min^{-1} under He-atmosphere

The three compounds are thermally stable below 300°C.

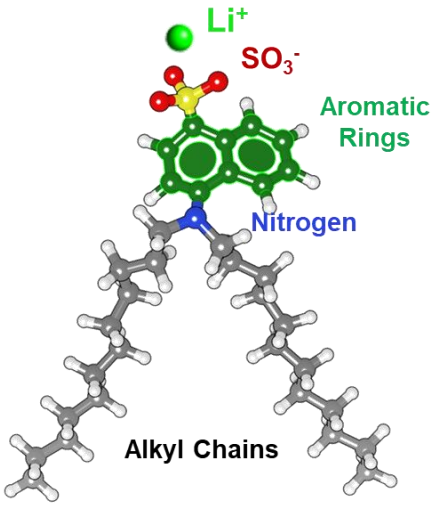

Figure S7: Ball and stick structure of the Liquid Crystal molecules with 12 alkyl groups in the chains (BS-Li-12).

Atoms	BS-Li-8	Atoms	BS-Li-12	Atoms	BS-Li-16
H (ring)	0.09432	H (ring)	0.09432	H (ring)	0.09432
C (ring)	-0.1494	C (ring)	-0.1494	C (ring)	-0.1494
C (ring)	-0.14346	C (ring)	-0.1435	C (ring)	-0.14355
C (ring)	-0.11709	C (ring)	-0.1171	C (ring)	-0.11718
H (ring)	0.10341	H (ring)	0.10341	H (ring)	0.10341
C (ring)	-0.07722	C (ring)	-0.0771	C (ring)	-0.07713
H (ring)	0.10008	H (ring)	0.10008	H (ring)	0.10008
C (ring)	-0.04464	C (ring)	-0.0444	C (ring)	-0.04446
H (ring)	0.14562	H (ring)	0.14562	H (ring)	0.14562
C (ring)	0.04149	C (ring)	0.04131	C (ring)	0.04131
C (ring)	0.13995	C (ring)	0.13977	C (ring)	0.13977
C (ring)	-0.56754	C (ring)	-0.5675	C (ring)	-0.56745
C (ring)	-0.18342	C (ring)	-0.1833	C (ring)	-0.18333
N	-0.47115	N	-0.4710	N	-0.47106
C (ring)	-0.05013	C (ring)	-0.0502	C (ring)	-0.05022
S	1.88235	S	1.88235	S	1.88235
H (ring)	0.10071	H (ring)	0.10071	H (ring)	0.10071
C (chain)	0.04212	C (chain)	0.04203	C (chain)	0.04203
C (chain)	0.04221	C (chain)	0.04212	C (chain)	0.04212
C (chain)	-0.17568	C (chain)	-0.1756	C (chain)	-0.17568
H (chain)	0.07236	H (chain)	0.07236	H (chain)	0.07236
H (chain)	0.07236	H (chain)	0.07236	H (chain)	0.07236
C (chain)	-0.1971	C (chain)	-0.1971	C (chain)	-0.1971
H (chain)	0.08469	H (chain)	0.08469	H (chain)	0.08469
H (chain)	0.08469	H (chain)	0.08469	H (chain)	0.08469
C (chain)	-0.14445	C (chain)	-0.1444	C (chain)	-0.14445
H (chain)	0.08073	H (chain)	0.08082	H (chain)	0.08073
H (chain)	0.08073	H (chain)	0.08082	H (chain)	0.08073
C (chain)	-0.13725	C (chain)	-0.1373	C (chain)	-0.13734
H (chain)	0.07893	H (chain)	0.07812	H (chain)	0.07893
H (chain)	0.07893	H (chain)	0.07812	H (chain)	0.07893
C (chain)	-0.153	C (chain)	-0.153	C (chain)	-0.153
H (chain)	0.07605	H (chain)	0.07605	H (chain)	0.07605
H (chain)	0.07605	H (chain)	0.07605	H (chain)	0.07605
C (chain)	-0.15138	C (chain)	-0.1513	C (chain)	-0.15174
H (chain)	0.07344	H (chain)	0.07335	H (chain)	0.07335

H (chain)	0.07344	H (chain)	0.07335	H (chain)	0.07335
C (chain)	-0.15516	C (chain)	-0.1550	C (chain)	-0.15507
H (chain)	0.07821	H (chain)	0.07812	H (chain)	0.07812
H (chain)	0.07821	H (chain)	0.07812	H (chain)	0.07812
C (chain)	-0.15309	C (chain)	-0.1528	C (chain)	-0.15282
H (chain)	0.07686	H (chain)	0.07677	H (chain)	0.07677
H (chain)	0.07686	H (chain)	0.07677	H (chain)	0.07677
C (chain)	-0.15066	C (chain)	-0.1542	C (chain)	-0.15426
H (chain)	0.07317	H (chain)	0.07299	H (chain)	0.07299
H (chain)	0.07317	H (chain)	0.07299	H (chain)	0.07299
C (chain)	-0.14688	C (chain)	-0.1498	C (chain)	-0.14985
H (chain)	0.07209	H (chain)	0.07191	H (chain)	0.07191
H (chain)	0.07209	H (chain)	0.07191	H (chain)	0.07191
C (chain)	-0.14949	C (chain)	-0.1528	C (chain)	-0.15282
H (chain)	0.07884	H (chain)	0.07839	H (chain)	0.07839
H (chain)	0.07884	H (chain)	0.07839	H (chain)	0.07839
C (chain)	-0.15003	C (chain)	-0.1525	C (chain)	-0.15255
H (chain)	0.07803	H (chain)	0.07758	H (chain)	0.07758
H (chain)	0.07803	H (chain)	0.07758	H (chain)	0.07758
C (chain)	-0.19251	C (chain)	-0.1537	C (chain)	-0.15372
H (chain)	0.07281	H (chain)	0.07425	H (chain)	0.07425
H (chain)	0.07281	H (chain)	0.07425	H (chain)	0.07425
C (chain)	-0.1908	C (chain)	-0.1496	C (chain)	-0.14967
H (chain)	0.07101	H (chain)	0.07254	H (chain)	0.07254
H (chain)	0.07101	H (chain)	0.07254	H (chain)	0.07254
H (chain)	0.06057	C (chain)	-0.1535	C (chain)	-0.15327
H (chain)	0.06057	H (chain)	0.07848	H (chain)	0.07848
H (chain)	0.06129	H (chain)	0.07848	H (chain)	0.07848
H (chain)	0.06129	C (chain)	-0.153	C (chain)	-0.15273
H (ring)	0.12276	H (chain)	0.07803	H (chain)	0.07794
H (chain)	0.06057	H (chain)	0.07803	H (chain)	0.07794
H (chain)	0.06129	C (chain)	-0.1521	C (chain)	-0.15426
O	-0.72117	H (chain)	0.07524	H (chain)	0.07515
O	-0.72117	H (chain)	0.07524	H (chain)	0.07515
O	-0.72117	C (chain)	-0.1503	C (chain)	-0.15228
		H (chain)	0.0738	H (chain)	0.0738
		H (chain)	0.0738	H (chain)	0.0738
		C (chain)	-0.1504	C (chain)	-0.15282
		H (chain)	0.07767	H (chain)	0.0774
		H (chain)	0.07767	H (chain)	0.0774
		C (chain)	-0.1499	C (chain)	-0.15201
		H (chain)	0.07731	H (chain)	0.07704
		H (chain)	0.07731	H (chain)	0.07704
		C (chain)	-0.1931	C (chain)	-0.15309
		H (chain)	0.07479	H (chain)	0.07596
		H (chain)	0.07479	H (chain)	0.07596
		C (chain)	-0.1930	C (chain)	-0.1521
		H (chain)	0.07407	H (chain)	0.07515
		H (chain)	0.07407	H (chain)	0.07515
		H (chain)	0.06219	H (ring)	0.12276
		H (chain)	0.06219	C (chain)	-0.14976
		H (chain)	0.06183	H (chain)	0.07542
		H (chain)	0.06183	H (chain)	0.07542
		H (ring)	0.12276	C (chain)	-0.15066
		H (chain)	0.06183	H (chain)	0.07569
		H (chain)	0.06219	H (chain)	0.07569
		O	-0.7211	H (chain)	0.07515
		O	-0.7211	C (chain)	-0.14904
		O	-0.7211	H (chain)	0.07515
				H (chain)	0.07551
				C (chain)	-0.1494
				H (chain)	0.07551
				H (chain)	0.07362
				H (chain)	0.07362
				C (chain)	-0.14895
				H (chain)	0.07371
				H (chain)	0.07371
				C (chain)	-0.14922
				H (chain)	0.07299
				C (chain)	-0.19071
				H (chain)	0.07299

				H (chain)	0.07335
				C (chain)	-0.1908
				H (chain)	0.07335
				H (chain)	0.06399
				H (chain)	0.06399
				H (chain)	0.06399
				H (chain)	0.06399
				H (chain)	0.06399
				H (chain)	0.06399
				O	-0.72117
				O	-0.72117
				O	-0.72117

Table S1: Per atom partial charge distribution for BS-Li-8, BS-Li-12, and BS-Li-16 as used in the MD simulations.

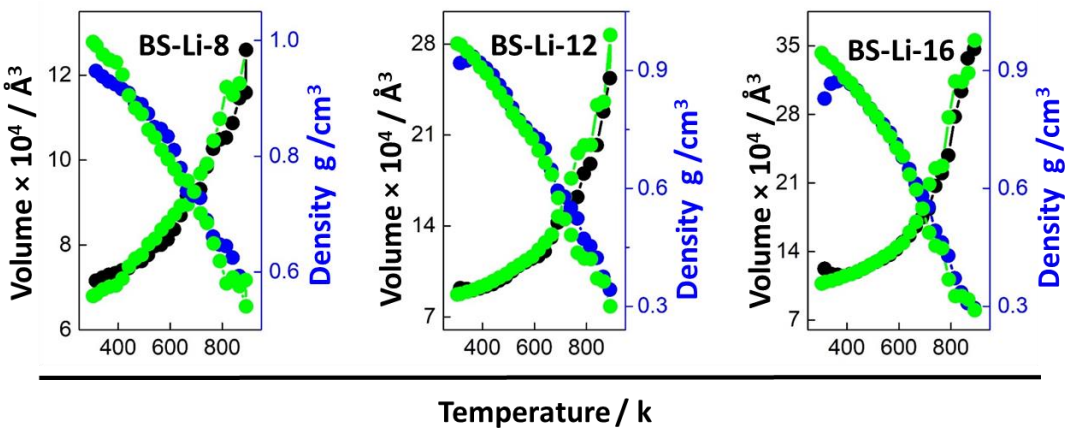

Figure S8: Change of the volume and density of the LC electrolytes as a function of the temperature. Volume (black), density (blue), and green for decreasing from high to lower temperature.

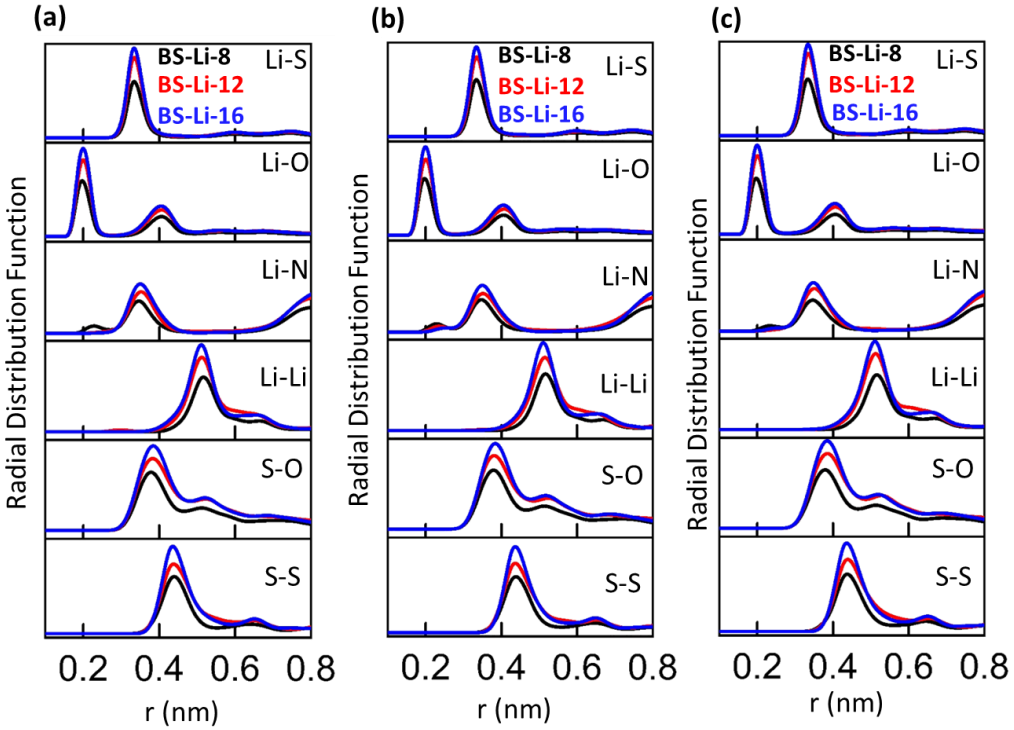

Figure S9: Simulated radial distribution function between Li-S, Li-O, Li-N, Li-Li, S-O, and S-N (a) in BS-Li-8 (black), BS-Li-12 (red), and BS-Li-16 (blue) at temperature 353 K (a), 373 K (b), and 393 K (c).

LCE	Li-S	Li-O	Li-N	Li-Li	S-O	S-S
BS-Li-8	0.33	0.19/0.40	0.23/0.34	0.52	0.38/0.52	0.44
BS-Li-12	0.33	0.20/0.40	0.35	0.51	0.38/0.52	0.44
BS-Li-16	0.33	0.20/0.40	0.35	0.51	0.38/0.52	0.44

Table S2: Summary of the RDF peak values for different correlations at temperature 353 K to 413 K.

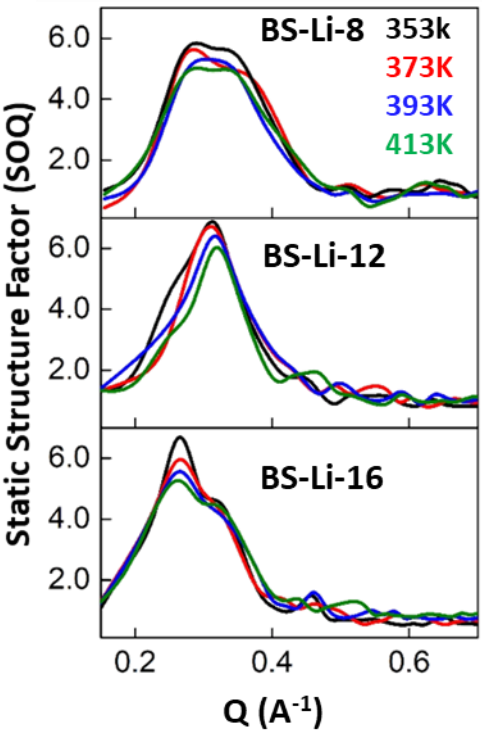

Figure S10: Simulated static structural factor of BS-Li-8, BS-Li-12, and BS-Li-16 at temperature 353 K (black), 373 K (red), 393 K (blue) and 413 K (green).

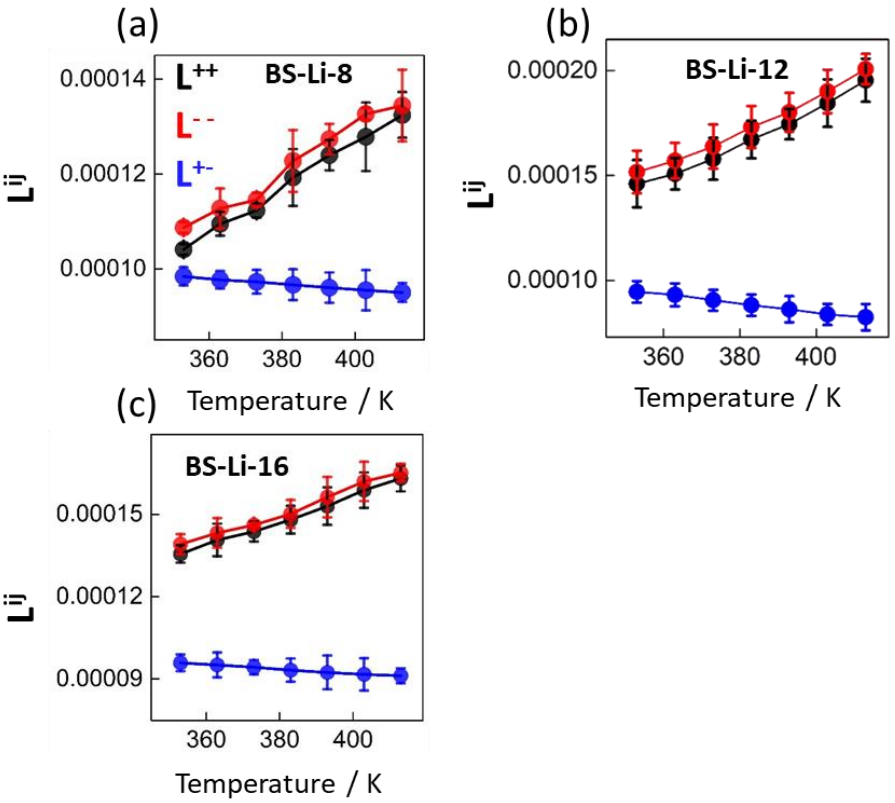

Figure S11: Onsager transport coefficients L^{++} (black), L^{--} (red), and L^{+-} (blue) of BS-Li-8 (a), BS-Li-12 (b), and BS-Li-16 (c) as a function of temperature.

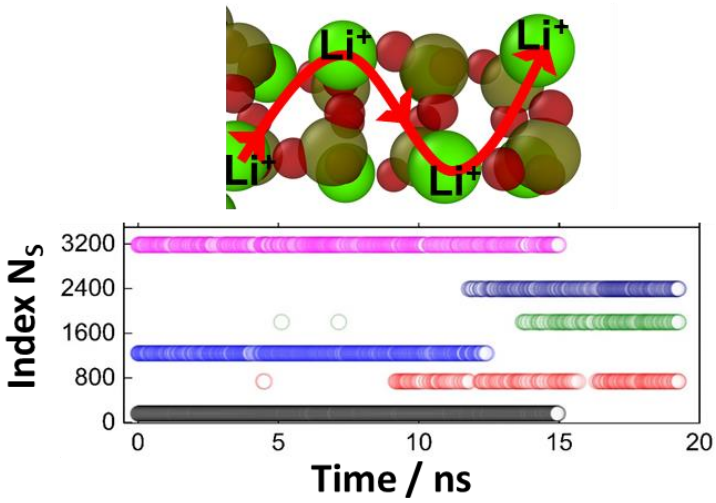

Figure S12: (a) Change of the S index of one Li^+ as a function of time in BS-Li-8. Index number of S (circle), (b) simulated illustration of the possible Li^+ conduction route. Alkyl chains of LC molecules were omitted for better clarity.

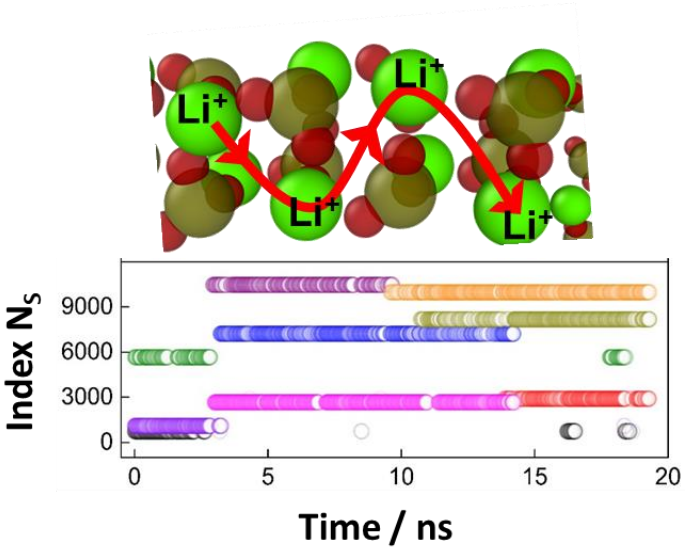

Figure S13: (a) Change of the S index of one Li^+ as a function of time in BS-Li-16. Index number of S (circle), (b) simulated illustration of the possible Li^+ conduction route. Alkyl chains of LC molecules were omitted for better clarity.